NASA Technical Paper 2773

December 1987

AD-A279 627

103626

Effect of Motion Cues During Complex Curved Approach and Landing Tasks

A Piloted Simulation Study

Charles H. Scanlon

NASA

NASA
Technical
Paper
2773

1987

Effect of Motion Cues During Complex Curved Approach and Landing Tasks

A Piloted Simulation Study

Charles H. Scanlon

Arkansas State University
State University, Arkansas

NASA

National Aeronautics
and Space Administration

Scientific and Technical
Information Division

Summary

A piloted simulation study was conducted to examine the effect of motion cues using a high-fidelity simulation of a commercial airplane during the performance of complex curved approach and landing tasks in the signal environment of the microwave landing system (MLS). The data from these tests indicate that in a high-complexity MLS approach task with moderate turbulence and wind, the pilot uses motion cues to improve path tracking performance. No significant differences in tracking accuracy were noted for the low- and medium-complexity tasks, regardless of the presence of motion cues. Higher control-input rates were measured for all the tasks when motion was used. Pilot eye scan, as measured by instrument dwell time, was faster when motion cues were used regardless of the complexity of the approach tasks. A pilot subjective rating, based on time load, mental effort load, and psychological stress load, yielded larger work load ratings with motion than with no motion. Pilot comments indicated that they preferred motion and that motion cues helped them accomplish their task, especially in turbulence and during the landing phase of the approach. With motion cues, pilots appeared to work harder in all levels of task complexity and to improve tracking performance in the most complex approach task.

Introduction

The National Airspace System Plan of the Federal Aviation Administration (FAA) currently calls for the present instrument landing system (ILS) to be replaced by the time-referenced scanning beam (TRSB) of the microwave landing system (MLS). The expanded signal coverage has the potential to support multiple, complex approach paths that can be used for noise abatement, obstacle clearance, airport capacity increases, vortex avoidance, and instrument approach capability to runways or landing pads that are not directly associated with the MLS facility (ref. 1).

The FAA and NASA have developed a joint research effort called the MLS Advanced Applications Program. This is a multiple-phase effort using both fixed-base and motion-base piloted airplane simulations to define envelopes of usable approach path geometry considering the flight instrumentation, path tracking performance, and pilot acceptance and work load. There is a concern that quantifiable and subjective parameters being used to indicate pilot acceptance and work load may be affected by motion, or lack of motion, sensed by the pilot. These effects must be defined so that valid comparisons may be made between motion-base and fixed-base simulation studies.

The literature on the effects of motion cues is voluminous with varying results. (See refs. 2 and 3.) Two studies that have looked at the effects of motion cues on instrument approach tasks are presented in references 4 and 5. These studies used high-fidelity commercial airplane simulators in instrument landing system (ILS) approach tasks. Parrish and Martin (ref. 4) found that there is no difference in pilot-performance measurements used between motion- and fixed-base operations. Comstock (ref. 5) reported that in an ILS approach task, no significant differences due to motion were found in glide slope and localizer errors; however, motion did make significant differences in pilot control activity and lookpoint scan patterns.

A piloted simulation test was conducted to determine the effects of motion cues on the specific parameters used to indicate pilot tracking performance, acceptance, and work load in the joint NASA and FAA study. These parameters included pilot comments, a subjective work load assessment technique (SWAT), pilot eye scan patterns of the instrument panel, path tracking performance, pilot control activity, and airplane state variables. Comparisons of these parameters were made on approach paths of low, medium, and high levels of difficulty conducted with and without motion, with and without turbulence, and with three different wind models. This report describes the test setup and procedures and discusses the test results.

Symbols and Abbreviations

ADI	attitude director indicator
AGL	above ground level
ANOVA	analysis of variance
ATC	air traffic control
DCA	Washington National Airport
DME	distance measuring equipment
df	degrees of freedom
F	F ratio
FAA	Federal Aviation Administration
HSI	horizontal-situation indicator
ILS	instrument landing system
MLS	microwave landing system
MS	mean square
NASA	National Aeronautics and Space Administration
p	probability

RAD	radius
RMI	radio magnetic indicator
RMS	root mean square
SWAT	subjective work load assessment technique (pilot rating of time load, mental effort load, and psychological stress load)
TRSB	time-referenced scanning beam
VMS	Visual/Motion Simulator
WAL	Wallops Flight Facility
WPT	way point
γ	flight path angle, deg

Simulator Description

This study was conducted in the Langley Visual/Motion Simulator (VMS), which is a six-degree-of-freedom, motion-base simulator capable of presenting realistic acceleration and attitude cues to the pilot. A general purpose, scientific mainframe computer with a nonlinear, high-fidelity digital representation of a McDonnell Douglas DC-9 airplane provided inputs to drive the VMS motion-base simulator. Audio cues for engine thrust and aerodynamic buffet were also provided. The simulator had a generic cockpit with conventional flight controls and instrumentation. The flight controls included a column and control wheel, rudder pedals, throttle, speed brake, and flap controls. Flight instrumentation included conventional flight and navigation instruments and engine instrumentation. A forward-looking out-the-window visual scene of the runway environment was provided to each pilot. The VMS facility is described in more detail in reference 6.

Flight Instrument Description

Figure 1 shows the arrangement of the flight instrument panel used during the evaluation tests. The flight instrumentation was arranged in a standard "T" format and, with several exceptions, functioned in a conventional manner. The top of the "T", from left to right, consisted of a combined airspeed/Mach indicator, the attitude director indicator (ADI), and the barometric altimeter.

The ADI contained a dual-cue flight director programmed to give commands to the pilot to track the vertical and lateral paths that lead to the runway. On the left side of the ADI was a fast/slow "bug" that indicated up to ±20-knot airspeed deviations from a reference speed set by the pilot on the airspeed/Mach indicator. The ADI also contained a lateral-path-deviation indicator with full-scale indications of ±1500 ft and a vertical-path-deviation indicator with full-scale indications of ±250 ft.

The vertical portion of the standard "T" was formed by the horizontal-situation indicator (HSI) centered below the ADI. The basic information displayed on this HSI was similar to that shown on a conventional HSI: a rotating compass rose indicated the magnetic heading of the airplane, and a course arrow indicated the direction and lateral displacement of the airplane relative to a desired track. The track angle of the desired course was also displayed digitally in the upper right corner of the HSI. The HSI also included a vertical-path-deviation indicator, a heading reference on the compass rose that could be manually set by the pilot, and a digital meter in the upper left corner of the HSI used to indicate the active way point number upon which the guidance algorithm computations were based.

The remaining basic flight instrumentation on the instrument panel included a vertical-speed indicator and a turn and bank indicator located below the altimeter. These instruments operated in a conventional manner. A DME indicator and a radio magnetic indicator (RMI) were located below the airspeed/Mach indicator. This DME indicator displayed slant range distance between the airplane and the DME ground facility collocated with the MLS azimuth antenna. The RMI displayed the relative bearing of the MLS ground-system azimuth antenna from the airplane.

A second DME indicator was located below the HSI. The distance shown on this instrument was the "along track" distance, which was computed by the guidance algorithm as the distance along the programmed path between the airplane and the approach path intercept point on the runway.

Two different annunciator lights were used to indicate changes in direction and flight path angle of the programmed path. A light centered over the ADI was illuminated 5 sec before the airplane was to begin a turn and was extinguished at the end of the turn. When no turn was programmed, the light was illuminated 5 sec before the airplane crossed a way point and was extinguished 10 sec after the way point was crossed.

The second annunciator light was located to the right side of the ADI adjacent to the vertical-path-deviation indicator. This light would blink for 5 sec when the vertical flight path angle of the programmed path changed more than 1°. The light was also continuously illuminated whenever the programmed path required a descent.

Path Definition and Guidance Algorithm Definition

The path definition and guidance algorithm used during these tests was the "circular-path fixed-radius" algorithm used in reference 7. This path definition and guidance algorithm defined the lateral path as a series of straight-line segments between way points connected with circular arcs of specified radii. The vertical path was a series of constant flight path angle segments. Flight path angle changes occurred only at way points and at the midarc point of the turns.

The path deviation information displayed to the pilot and used in the guidance algorithm is illustrated in figure 2. (This figure corresponds to a 90° right turn with a flight path angle change.) The vertical profile view shows that the vertical transition from the level-flight inbound path segment to the 3.1° descent on the outbound path segment occurred when the airplane passed the midarc point of the turn. Vertical path deviations and flight director commands displayed to the pilot were smooth and continuous during the vertical transition.

Lateral path deviations and flight director steering commands during the turns were computed based on tracking circular paths with turn radii defined in the approach procedure. Lateral deviations were computed as the distance between the airplane and the path along a line that passed through both the turn center and the airplane. The intersection of this line with the circular arc was called the abeam point. The tangent to the path at the abeam point defined the desired path track angle for the airplane to fly during the turn. All lateral path deviations and steering commands were smooth and continuous throughout the turns.

The HSI was interfaced with the guidance algorithm so that track angles and course deviations could be presented. The algorithm computed and continuously displayed the desired track angle as illustrated in figure 2(c). Lateral and vertical deviations were displayed with the same ±1500-ft lateral limit and ±250-ft vertical limit used on the ADI.

The guidance algorithm also drove a bearing pointer arrow on the HSI to indicate the desired course at the end of the turn. At 5 sec before the airplane was to begin a turn, the arrow would be driven to the track angle of the next leg, thus giving the pilot a pictorial view of where he would be rolling out of the turn. The arrow would remain in that position until the beginning of the next turn.

Approach Tasks and Instrument Procedures

Three different combinations of approach paths and guidance were used during these evaluation tests to simulate low-, moderate-, and high-complexity approach tasks. One approach was designed to emulate a typical ILS approach with flight director guidance and was used as the low-complexity approach task. The moderate-complexity curved approach task had multiple turns and one flight path angle change with flight director guidance provided. The high-complexity curved approach task had multiple turns and flight path angle changes and was flown without the aid of flight director commands.

An out-the-window visual scene presented a gray cloud picture down to a height of 200 ft above ground level (AGL). At the 200-ft level, a terrain scene with a simulated 1/2-mile visibility was presented to aid the subject in landing.

The subject pilots were given the task of following the path on instruments down to a decision height of 200-ft AGL, and then of making a normal landing, if possible. The subject pilots were instructed to make a go-around if a normal landing was not possible. Other pilot duties included responding to ATC communications, tuning the communications transceiver, operating the transponder, and configuring the airplane for landing.

SLINE Approach

The straight-line (SLINE) approach task shown in figure 3 was chosen to replicate a typical ILS approach. This approach, flown with flight director commands, represented the lowest level of task complexity. The path had a constant flight path angle of 3° and a constant track angle of 212°.

The flight was initially positioned 2 n.mi. laterally offset from a point on the runway centerline that was 12.7 n.mi. from the touchdown point. Initial indicated airspeed was set at 210 knots, altitude at 2200 ft, and heading at 182°.

The subject pilot was given the assignment of maintaining initial heading and altitude until established on the path laterally and vertically, respectively. Once established on this path, the subject then proceeded as in a normal ILS approach.

RIVER Approach

The RIVER approach shown in figure 4 was flown with flight director steering commands and represented the medium-complexity approach task. The approach path geometry is the same as the RIVER approach (ref. 8) into Washington National Airport (DCA) except that it has been oriented to runway 22 at the NASA Wallops Flight Facility (WAL). The path was chosen because the large number of turns

that occur in a short distance increased the complexity as compared with the SLINE approach. The airplane was initialized on the path at way point WPT01 with an initial airspeed of 210 knots in straight and level flight.

HOOK Approach

The HOOK approach shown in figure 5 was flown without flight director steering commands and was the most complex approach task. The three turns and three flight path angle changes flown with raw data made this the most complex task. Initially, the airplane was positioned so that it was heading along the path at WPT01 with an indicated airspeed of 250 knots.

Test Design

These simulator tests were designed to study the effects of motion cues on pilot performance and work load during flight along various levels of MLS approach task complexity. This study was accomplished through the evaluation of tracking performance, pilot control activity, subjective work load ratings, pilot scan behavior, and pilot comments for three levels of task complexity. Since pilot fatigue is an operational reality, it was felt that pilot fatigue should be induced during these tests. This fatigue was accomplished by scheduling the 36 runs plus any necessary reruns during a 2-day period and by allowing few rest breaks.

Test Matrix

Three approach tasks flown with and without turbulence, with and without motion, and with three wind models resulted in a $3 \times 2 \times 2 \times 3$ matrix of runs. The runs were arranged in the random order shown in table I and were flown in that order by four of the test subjects, and then in the reverse order by the remaining three test subjects.

Turbulence accelerations along each of the three axes were generated by a Dryden spectoral form used in a statistical model. An RMS gust intensity of 4 ft/sec was used as an input to derive the simulated moderate turbulence.

Three wind models were used in the test matrix. Wind model 0 had a velocity of 0 at all altitudes. The first nonzero wind model, wind model 1, resulted in a surface wind of 15 knots at 272°. This simulated a 60° right crosswind on landing. Wind direction increased 10° and windspeed increased 5 knots per 1000 feet above the runway. Wind model 2 resulted in a surface wind of 15 knots at 152°. This was a 60° left crosswind to the runway. Wind direction decreased 10° and windspeed increased 5 knots per 1000 feet above the runway. Only surface wind conditions were given each test subject before each run.

ATC Communications

Air traffic control (ATC) communications were provided to enhance the realism of the simulation and to provide a secondary task by playing 12 prerecorded audio tapes. The tapes included one-way communications with the test subject and two-way communications with other simulated airplanes. Each tape was time coordinated to one of the three approach tasks so that relevant messages would transpire at a timely airplane position in that approach. Each tape contained five to six messages relevant to the test subject, two of which required pilot action of radio tuning, transponder changes, or verbal reports.

SWAT

A subjective work load assessment technique (SWAT) (ref. 9) was used to quantify pilot assessments of work load. This technique is a three-step process consisting of a pilot rating for each run, a scale development phase, and a translation of each pilot rating into a single work load measure. At the end of each data run, subject pilots gave subjective ratings for that run using three work load measures: time load, mental effort load, and psychological stress load. Each measure was rated using a number from 1 to 3 including fractional values, as defined in table II.

In the scale development phase, each subject sorted a deck of cards in the order of his perceived work load. Each card had one of the three levels of assessment for each of the three work load measures, as defined in table II. This gave a total of $3 \times 3 \times 3 = 27$ cards. The cards were then used to develop a percentage scale so that pilot SWAT ratings could be translated into a single percentage rating for each run (ref. 9).

The last phase consisted of quantification of the pilot ratings. The group scale developed above was used to translate the three numerical ratings for each run into a single work load measure from 0 (the lowest) to 100 (the highest) work load measure. A linear interpolation process was used for the fractional ratings.

Test Subjects

Seven subject pilots were used in these tests. Four of these pilots were employed as management or training pilots for an airline. Each of these pilots flies actively for their company. Two of the subjects were active-duty, jet-transport pilots in the U.S. Air

Force. A NASA research pilot was also used as a test subject. All the test subjects had experience in jet-transport airplanes.

Test Procedures

The test period for each subject consisted of 3 consecutive days. The first day was used for pilot briefing, SWAT card sorting, and flying familiarization runs. The next 2 days were used for flying the test matrix shown in table I.

The briefing period lasted about 2 hr. The subject pilots were informed on airplane performance (including airspeed, flap, and gear operation limitations), instrument configuration and display, and airplane operating procedures. The ATC communications and expected pilot responses were discussed. Approach procedures and operational strategies for flying the airplane were discussed.

During the familiarization period, each pilot flew a minimum of 13 runs along each of the three approach paths. Three of the HOOK approaches were flown with the aid of a flight director so that the pilot could form a base reference for pitch and bank attitudes to use during the data runs. Four other HOOK practice approaches and all HOOK data approaches were flown without the flight director. Turbulence, motion, and wind were also varied on or off during this period. The simulation could be stopped and then continued if the pilot had questions about the run. Additional familiarization runs were conducted if the subject pilot desired them.

Test runs for recorded data began in the morning of the second day. Each test run was begun with the airplane established in a trimmed, straight and level attitude. The pilot was told that he should complete the approach and land if possible, but he was to execute a missed approach if he did not feel that the airplane was stabilized or in a position from which a landing could be made.

The test conductor functioned as copilot during the test runs and performed normal copilot duties including calling checklists, selecting flaps and gear on the subject's command, and giving the pilot verbal "call outs" when the airplane was 1000 ft AGL, 500 ft AGL, 300 ft AGL, and when the decision height of 200 ft AGL was reached. He also called attention to abnormal flight conditions such as excessive vertical speeds, high or low airspeeds, and excessive path tracking errors. After each run the test conductor would record pilot SWAT ratings and comments.

Recorded Data

Data recorded for each test run include the following: digital data that describe the state of the airplane, path tracking parameters, and flight control activity at a 5.33-Hz sample rate; scan behavior measures at a 32-Hz rate; video images of the pilot's lookpoint superimposed on the instrument panel; pilot comments during and after each approach; pilot responses to ATC communications; and SWAT ratings.

Oculometer

Pilot scan behavior was measured by the oculometer system at the Langley Research Center. This oculometer is a highly modified version of the Honeywell Mark 3A remote oculometer (ref. 10) that allows head movement by a subject of up to 1 ft^3. The system operates by projecting a beam of collimated infrared light at one of the subject's eyes. Two reflections are returned to a video camera. The first is a broad (4- to 8-mm) reflection of the retina, bounded by the pupil, like a cat's eye reflecting from the headlight of a car; the second is an intense pinpoint reflection from the surface of the cornea. From the video signals of the eye's reflections, the computer calculates the pilot's foveal lookpoint on the instrument panel. A video tape of the instrument panel and the pilot's superimposed lookpoint was saved as a permanent record of the test. The lookpoint coordinates and pupil diameter are recorded at each computer iteration for later analysis.

Method of Analysis

Data were recorded on more than 252 test runs during this study. The data from each test run were statistically reduced and then compiled into a general data base. Data sets, used for comparison purposes, could then be generated from the general data base. Data sets were generated for each of the three levels of difficulty of the approach task, for motion and no motion, for turbulence and no turbulence, and for each of the three wind models used in the simulation. Since reruns were necessary because of occasional component failure, care was taken to ensure that data sets used in the comparisons were balanced (i.e., a similar proportion of the subject pilots, wind and turbulence conditions, types of approach paths, etc.) to preclude artificially skewing the results of the comparisons.

Specific data used to evaluate path tracking performance, airplane state, and pilot control inputs included lateral and vertical path deviations, track angle error, flight path angle error, vertical speed, airspeed, airplane configuration, and pilot control position. Statistical analysis included computing the mean, the standard deviation, the root mean square, and the mean rate of change for each of these

recorded variables for each run and for subsets of the general data base when used in comparative analyses.

An indication of physical work load was identified through pilot control activity. A column, wheel, or throttle input was defined as a movement of more than 0.1° during one data-recording iteration (0.1875 sec). A reversal was defined as an input in the opposite direction from the last input (i.e., from a push to a pull on the column or throttle or a right to left movement of the wheel). Input and reversal rates for the column, wheel, and throttle were computed for each run and for each subset of runs used in the comparative discussions.

Since this experiment was a within-subjects factorial design, a rectangular array of data sets was formed by taking one data set for each of the 36 runs for each of the 7 subject pilots. In the case of repeated runs due to system failures, the first run with valid data was included; and in the case of a missing or bad data run, mean values of the other pilots were used. This procedure resulted in a 36 × 7 matrix of test runs that was used in analysis of variance tests (ref. 11) on the recorded data.

Eye-scan-behavior data reduction included computing the mean dwell time on each instrument, the percentage of total time spent looking at each instrument, the percentage of eye movement transitions between pairs of instruments, and the mean transitions per second for each run. The data sets were divided by path, motion, turbulence, and wind models. Expected values and standard errors of the means were then computed. Standard t-tests were used in comparative analyses of the different conditions.

Results and Discussion

A comparison is needed to determine how conclusions based on complex MLS approach test results in a fixed-base simulator would differ from conclusions based on complex MLS approach test results in a motion-base simulator. The purpose of this comparison is to determine the effect of motion cues on simulated complex MLS approach tasks.

Tracking Data Comparison

To determine the effects of motion cues on tracking performance, analysis of variance (ANOVA) tests using the 36 × 7 matrix described in the "Method of Analysis" section were conducted for tracking performance variables including the root-mean-square (RMS) lateral and vertical deviations from the approach path for each run. Also, to further measure the differences obtained, the mean, the root mean square, and the standard deviation of the tracking performance variables were computed by averaging across all pilots, and the subsets were formed by subdividing the complete performance data set by task complexity, turbulence, wind, and motion.

Table III presents the results of the ANOVA test used on RMS lateral deviation. As illustrated for CM, CT, and CW, motion did have a statistically significant effect in its second-order interaction with task complexity ($p = 0.0236$), with turbulence ($p = 0.0333$), and with wind ($p = 0.041$), respectively. The main effect of motion, however, was not detected to be statistically significant by itself. Other measurable higher order interactive effects involving motion were

$$\text{CMT} = \text{Complexity} \times \text{Motion} \times \text{Turbulence} \qquad (p = 0.0054)$$

$$\text{CMW} = \text{Complexity} \times \text{Motion} \times \text{Wind} \qquad (p = 0.0085)$$

$$\text{CMTW} = \text{Complexity} \times \text{Motion} \times \text{Turbulence} \times \text{Wind} \qquad (p = 0.0061)$$

To illustrate the effects of motion and task complexity on lateral errors, RMS lateral deviations were computed for subsets formed by grouping the entire performance data set by the three levels of task complexity and by having motion and no motion. These values are graphed in figure 6.

For the RIVER and SLINE approach tasks, motion cues did not have an operationally significant effect on RMS lateral deviation because the differences were less than 10 ft in each comparison. However, motion did have a significant operational effect on RMS lateral deviation in the HOOK approach task where motion resulted in a 427.5-ft deviation and no motion resulted in a 515.5-ft deviation. Thus, the effects of motion on lateral tracking error were only operationally significant in the highest complexity approach task.

The effects of motion cues in relation to wind and task complexity on RMS lateral deviation are illustrated in figure 7, in which the wind case included the two nonzero wind models and the no-wind case had zero wind velocity at all altitudes. The largest difference in the motion/no-motion comparisons was in the HOOK approach task with wind, where the RMS lateral deviation with no motion was 558.6 ft versus the motion case of 473.8 ft. Even the no-wind case for the HOOK approach task resulted in a 59.0-ft difference with a no-motion value of 363.7 ft and a motion value of 304.7 ft. For the moderate- and low-complexity approach tasks, motion/no-motion comparisons yielded less than a 25-ft difference in both the wind and no-wind cases.

Motion effects on RMS lateral deviations for turbulence and no turbulence are graphed for each of the three levels of task complexity in figure 8. Motion was only operationally significant in the case of

the HOOK approach task with turbulence in which motion cues resulted in a lateral RMS error of 402.7 ft versus the no-motion case that resulted in an RMS error of 526.9 ft. In each of the other comparisons in this figure, the differences were less than 25 ft. Thus, motion was only operationally significant in the presence of turbulence in the most complex approach task.

Figure 9 further illustrates the effects of motion on the most complex approach task. Here, the set of HOOK approaches was subdivided by motion and no motion, turbulence and no turbulence, and wind and no wind, thus resulting in eight data sets from which RMS lateral errors were computed. In three of the four comparisons of motion versus no motion, the no-motion case resulted in a larger error. The largest difference was in the turbulence-wind case where no motion resulted in an error of 697.5 ft versus the motion case that resulted in an error of 481.5 ft.

Although the analysis of variance (ANOVA) test on the RMS vertical deviation did reveal significant differences due to the main effects of task complexity and turbulence, no conclusions were found for motion. The results of the ANOVA test, as presented in table IV, do not show any significant difference because of the main effect of motion or its interaction with any combination of the other main factors. Comparisons of the effects of motion versus no motion yielded RMS vertical tracking-error differences of less than 20 ft for each of the three approach task complexities.

Further statistical analysis of other path tracking variables revealed some minor differences. The motion case resulted in slightly higher values than the no-motion case of RMS flight path angle error, rate of change of flight path angle error, and rate of change of altitude error, with a value of p less than 0.01 in each case.

In summary, with motion cues, smaller lateral tracking errors resulted for the most complex approach task when wind and turbulence were present. Differences due to motion in vertical tracking errors (for all levels of task complexity) and in lateral tracking errors (for the medium- and low-complexity tasks) were not statistically or operationally significant.

Pilot-Control-Activity Comparisons

For a comparison of pilot control activity with motion versus pilot control activity without motion, analysis of variance (ANOVA) tests were run for pilot-activity measures including column-input rate, wheel-input rate, and throttle-input rate. Also, average column-, wheel-, and throttle-input rates were computed for data sets grouped according to task complexity, motion, turbulence, and wind.

Table V summarizes the analysis of variance test for pilot column-input activity. These results revealed that motion had a strong significance ($p = 0.0019$) on the pilot column-input rate throughout the data matrix. Also, there was a significant interaction effect between motion and turbulence with a value of p of 0.0175.

To illustrate the effects of motion and the interaction of motion with turbulence, column-input rates were computed for subdivisions of the performance data set formed by sorting the three levels of task complexity with motion and no motion and with turbulence and no turbulence. This computation yielded the 12 values plotted in figure 10. The motion cases resulted in larger column-input rates than the no-motion cases in each of the six comparisons, although the difference in the case of the RIVER approach task with no turbulence was not statistically significant. Motion made a larger and more consistent difference in the turbulence cases than in the no-turbulence cases.

The effect of motion on the average pilot wheel-input rates was also statistically significant. Table VI presents the results of the ANOVA test for the wheel-input rates. As can be seen, motion had a strong significant effect ($p = 0.0004$) throughout the data matrix. There were no interaction effects with any combination of the other factors.

Figure 11 presents the differences between the pilot wheel-input rates for the motion and no-motion cases. Motion resulted in larger wheel-input rates than no motion in each of the comparisons using task complexity. The differences appear to be fairly uniform across task complexity, which might explain the large statistical significance ($p = 0.0004$). From an operational point of view, motion appears to have only a slight significance.

Pilot throttle-input rates were also tested by analysis of variance methods, and the results are presented in table VII. As can be seen, the data did not reveal any conclusions about motion or its interaction with any combination of the other factors.

Statistical analysis of pilot column-reversal rates, wheel-reversal rates, and throttle-reversal rates produced no additional information. Consequently, those analyses are not presented here.

In summary, motion cues yielded a higher physical work load as measured by pilot control activity. With motion, higher wheel- and column-input rates were measured for all levels of task complexity.

SWAT Comparisons

The analysis of variance test results for the SWAT data matrix did show a slight significance due to motion. Table VIII illustrates that the main effect of motion and the interaction effect of motion and turbulence were marginally significant with values of p of 0.0527 and 0.0475, respectively.

To illustrate the motion effects, the SWAT data set was divided by task complexity, motion, and turbulence, and the mean values were computed. In the results displayed in figure 12, the subject pilots rated the motion cases higher than the no-motion cases for each of the three approach tasks when turbulence was present. Mixed results were obtained in the no-turbulence cases, as illustrated.

Scan Behavior Comparisons

Statistical analysis of the scan behavior data set included computing (for each test run) the mean dwell time at each instrument position, the percentage of dwell time at each instrument position, the transition percentages between instrument pairs, and the mean transitions per second. Standard t-tests were used in comparing subsets of the data set formed from sorting by the three task complexities and by having motion and no motion.

Figure 13 illustrates the 14 instrument look areas that were defined for statistical analysis of the oculometer data. The attitude indicator had five distinguishable look areas: the center that included the artificial horizon and flight director bars, the upper part that contained the bank angle pointer, the right part that had a vertical deviation/glide slope needle, the bottom part that contained the lateral deviation/localizer needle, and the left part that contained the airspeed deviation indicator. The engine instruments were grouped into one classification area, and the rest of the instruments were identified as individual areas without subdividing or grouping.

Shorter statistically significant mean dwell times were recorded in the motion case than in the no-motion case for the following instrument look areas: for the HOOK approach task—glide slope needle, bank angle pointer, turn/way point annunciator, and slant range DME; for the RIVER approach task—localizer needle, glide slope needle, and the turn/way point annunciator; and for the SLINE approach task—glide slope needle, artificial horizon/flight director bars, bank angle pointer, turn/way point annunciator, and barometric altimeter. The SLINE results reinforce those presented by Comstock in reference 5.

In the motion versus no-motion comparisons, no conclusions were evident when comparing the percentage of dwell time at each instrument position or the percentage of transitions between pairs of instrument positions.

Pilot Comments

This section summarizes comments made by the subject pilots. Comments were recorded by the test conductor during each run and immediately after the SWAT rating at the end of each run.

All pilots indicated a preference for motion over no motion. Pilots stated that "motion gives you a sense of feel" and "without motion, you lose some of the realism needed to get a better perspective of what's occurring." Several pilots felt that the approaches were "a little unrealistic" and "a little more artificial" without motion.

Two pilots indicated that different visual instrument scan techniques were needed in the motion versus no-motion cases. One stated that a lack of motion "forced me to change my scan." Another added that "without motion, you need a faster scan, and I don't have one." Both comments were made immediately after a HOOK approach with turbulence, wind, and no motion.

Six pilots indicated that they believed that motion made it easier to fly a good approach. Comments included: "It's more difficult without motion," "... harder to do without motion," "Motion helps get rid of stress and work load," and "The absence of motion made it more difficult."

A lot of the pilot comments indicate a strong belief that motion helps make turbulence easier to deal with. Typical comments included: "Turbulence is disconcerting without motion," "Turbulence doesn't appear to be as significant with no motion as it does with motion," and "Turbulence is hard to deal with when you don't feel it."

The awareness of motion by the test subjects appeared to be largest at the beginning of each run and when on visual flight by terrain features. Comments included: "Motion is missed especially on visual [flight]," "[The airplane] lands a lot easier with motion," "[I] did not notice motion until visual reference," and "I only noticed motion at the beginning and end of the run."

One pilot stated that "without motion, I'm content to let it [a small course deviation] go rather than correct." This may partially explain why the pilots worked harder, as measured by SWAT, control activity, and instrument dwell times, but commented that

flying a good approach was easier with the addition of motion cues. With motion cues it appears that the subjects were stimulated to work harder to do a better job.

In summary, the subject pilots preferred to fly with motion. Most felt that motion helped them accomplish their task, especially in turbulence and when landing. Some also believed that motion cues made it easier to fly a good approach. Thus, motion cues appear to stimulate the pilots to work harder to fly a better approach.

Concluding Remarks

NASA utilizes both fixed-base and motion-base piloted simulation facilities in the conduct of its flight research. One multiphase research program concerned with flight operations within the microwave landing system coverage uses both fixed-base and motion-base airplane simulators to define envelopes of usable approach path geometry. There was concern during this program that both the quantitative and subjective measures being used to indicate pilot performance, acceptance, and work load might be affected by motion, or lack of motion, as sensed by the pilot. This concern led to an additional study, the objective of which was to determine the effects of motion cues during manually flown, curved approach and landing tasks.

During this study seven subject pilots flew a test matrix of 36 approach and landing tasks in a high-fidelity motion-base airplane simulator equipped with electromechanical flight displays. The test matrix contained three approach paths of high, medium, and low complexity, with and without turbulence, with and without motion, and with three different wind models. Recorded parameters included pilot comments, subjective work load assessment technique (SWAT) ratings (a pilot rating of time load, mental effort load, and psychological stress load), pilot eye scan patterns of the instrument panel, path tracking performance, flight control activity, and airplane state variables. Analysis of variance (ANOVA) tests were conducted on path tracking performance and on pilot work load measures, and statistical summaries of subsets of the data set were compared to determine the effects of motion.

It was concluded from this study that although the pilot does use cues from motion, tracking performance results obtained with a fixed-base simulation are comparable to those obtained in a motion-base simulation for approach tasks of low-to-moderate complexity. However, during high-complexity approach tasks, lateral tracking errors are larger when motion cues are not present. Vertical tracking errors were not significantly affected by the presence or absence of motion cues in any of the cases tested.

The subject pilots indicated that they preferred motion and that motion cues helped them accomplish their task, especially in turbulence and during the landing phase of the approach. The data showed that when motion cues and turbulence were present, higher SWAT ratings, shorter eye scan (as measured by instrument dwell time), and higher control wheel and column activity resulted in all levels of approach task complexity.

NASA Langley Research Center
Hampton, VA 23665-5225
November 9, 1987

References

1. *Getting Ready for MLS.* U.S. Dep. of Transportation, Jan. 1985.
2. Puig, Joseph A.; Harris, William T.; and Ricard, Gilbert L.: *Motion in Flight Simulation: An Annotated Bibliography.* Rep. No. NAVTRAEQUIPCEN IH-298, U.S. Navy, July 1978.
3. Gibino, Dominick J.: *Effects of Presence or Absence of Cockpit Motion in Instrument Flight Trainers and Flight Simulators.* ASD-TR-68-24, U.S. Air Force, June 1968. (Available from DTIC as AD 675 543.)
4. Parrish, Russell V.; and Martin, Dennis J., Jr.: *Comparison of a Linear and a Nonlinear Washout for Motion Simulators Utilizing Objective and Subjective Data From CTOL Transport Landing Approaches.* NASA TN D-8157, 1976.
5. Comstock, James R., Jr.: *Oculometric Indices of Simulator and Aircraft Motion.* NASA CR-3801, 1984.
6. Parrish, Russell V.; and Bowles, Roland L.: *Motion/Visual Cueing Requirements for Vortex Encounters During Simulated Transport Visual Approach and Landing.* NASA TP-2136, 1983.
7. Knox, Charles E.: *Flying Complex Approach Paths Using the Microwave Landing System.* SAE Tech. Paper Ser. 861771, Oct. 1986.
8. *United States Government Instrument Approach Procedures, U.S. Southeast, Volume 1.* U.S. Dep. of Commerce, May 1987.
9. Reid, Gary B.; Shingledecker, Clark A.; Nygren, Thomas E.; and Eggemeier, F. Thomas: Development of Multidimensional Subjective Measures of Workload. *Proceedings International Conference on Cybernetics and Society*, IEEE Catalog No. 81CH1683-2, IEEE Systems, Man and Cybernetics Soc., c.1981, pp. 403 406.
10. Harris, Randall L., Sr.; Glover, Bobby J.; and Spady, Amos A., Jr. (appendix A by Daniel W. Burdette): *Analytical Techniques of Pilot Scanning Behavior and Their Application.* NASA TP-2525, 1986.
11. Winer, B. J.: *Statistical Principles in Experimental Design, Second ed.* McGraw-Hill Book Co., Inc., c.1971.

Table I. Test Matrix

Run	Approach path	Turbulence	Motion	Wind model
1	RIVER	Off	Off	0
2	SLINE	Off	On	2
3	RIVER	On	Off	1
4	SLINE	On	On	0
5	HOOK	Off	Off	2
6	SLINE	On	Off	1
7	RIVER	Off	On	0
8	HOOK	On	On	2
9	RIVER	On	On	1
10	HOOK	Off	On	0
11	HOOK	On	Off	2
12	SLINE	Off	Off	1
13	HOOK	Off	Off	1
14	SLINE	On	Off	0
15	RIVER	Off	On	2
16	HOOK	On	On	1
17	RIVER	On	On	0
18	HOOK	Off	On	2
19	HOOK	On	Off	1
20	SLINE	Off	Off	0
21	RIVER	Off	Off	2
22	SLINE	Off	On	1
23	RIVER	On	Off	0
24	SLINE	On	On	2
25	RIVER	On	On	2
26	HOOK	Off	On	1
27	HOOK	On	Off	0
28	SLINE	Off	Off	2
29	RIVER	Off	Off	2
30	SLINE	Off	On	0
31	RIVER	On	Off	2
32	SLINE	On	On	1
33	HOOK	Off	Off	0
34	SLINE	On	Off	2
35	RIVER	Off	On	1
36	HOOK	On	On	0

Table II. SWAT Rating Chart

Time load may be rated on the three-point scale below: (1) Often have spare time. Interruptions or overlap among activities occur infrequently or not at all. (2) Occasionally have spare time. Interruptions or overlap among activities occur frequently. (3) Almost never have spare time. Interruptions or overlap among activities are very frequent, or occur all the time.
Mental effort load may be rated using the three-point scale below: (1) Very little conscious mental effort or concentration required. Activity is almost automatic, requiring little or no attention. (2) Moderate conscious mental effort or concentration required. Complexity of activity is moderately high due to uncertainty, unpredictability, or unfamiliarity. Considerable attention required. (3) Extensive mental effort and concentration are necessary. Very complex activity requiring total attention.
Psychological stress load may be rated on the three-point scale below: (1) Little confusion, risk, frustration, or anxiety exists and can be easily accommodated. (2) Moderate stress due to confusion, frustration, or anxiety noticeably adds to work load. Significant compensation is required to maintain adequate performance. (3) High to very intense stress due to confusion, frustration, or anxiety. High to extreme determination and self-control required.

Table III. Results of ANOVA Test on RMS Lateral Deviation

[C: task complexity; M: motion; T: turbulence; W: wind]

Source	df	MS	F	p
C	2,12	4 098 273	57.70	0.0000
M	1,6	37 987	3.68	
T	1,6	51 109	3.44	
W	2,12	130 981	19.85	.0002
CM	2,12	30 515	5.20	.0236
CT	2,12	19 268	2.56	
CW	4,24	93 352	14.75	.0000
MT	1,6	37 039	7.57	.0333
MW	2,12	18 905	4.22	.0410
TW	2,12	2 421	.16	
CMT	2,12	27 662	8.33	.0054
CMW	4,24	25 689	4.37	.0085
CTW	4,24	5 462	.37	
MTW	2,12	11 191	2.46	
CMTW	4,24	25 915	4.69	.0061

Table IV. Results of ANOVA Test on RMS Vertical Deviation

[C: task complexity; M: motion; T: turbulence; W: wind]

Source	df	MS	F	p
C	2,12	100 745.1	56.17	0.0000
M	1,6	149.6	.58	
T	1,6	3 324.5	56.91	.0003
W	2,12	191.8	1.36	
CM	2,12	30.5	.21	
CT	2,12	706.8	3.09	
CW	4,24	627.8	2.94	.0414
MT	1,6	2 130.9	2.02	
MW	2,12	597.9	2.84	
TW	2,12	847.3	4.60	.0328
CMT	2,12	951.5	1.77	
CMW	4,24	374.1	.81	
CTW	4,24	632.6	1.66	
MTW	2,12	642.2	1.99	
CMTW	4,24	965.6	2.48	

Table V. Results of ANOVA Test on Column-Input Rate

[C: task complexity; M: motion; T: turbulence; W: wind]

Source	df	MS	F	p
C	2,12	0.464	11.02	0.0019
M	1,6	1.918	27.61	.0019
T	1,6	8.826	74.87	.0001
W	2,12	.139	3.77	.0535
CM	2,12	.121	3.04	
CT	2,12	.281	3.60	.0596
CW	4,24	.085	1.66	
MT	1,6	.680	10.54	.0175
MW	2,12	.031	1.42	
TW	2,12	.002	.03	
CMT	2,12	.145	2.44	
CMW	4,24	.016	.19	
CTW	4,24	.110	1.24	
MTW	2,12	.041	.61	
CMTW	4,24	.090	2.17	

Table VI. Results of ANOVA Test on Wheel-Input Rate

[C: task complexity; M: motion; T: turbulence; W: wind]

Source	df	MS	F	p
C	2,12	0.544	9.78	0.0030
M	1,6	1.630	52.31	.0004
T	1,6	17.495	68.71	.0002
W	2,12	.185	2.61	
CM	2,12	.010	.10	
CT	2,12	2.431	32.92	0.0000
CW	4,24	.024	.42	
MT	1,6	.050	1.12	
MW	2,12	.060	1.85	
TW	2,12	.094	1.97	
CMT	2,12	.011	.13	
CMW	4,24	.052	.88	
CTW	4,24	.056	.73	
MTW	2,12	.022	.20	
CMTW	4,24	.131	1.80	

Table VII. Results of ANOVA Test on Throttle-Input Rate

[C: task complexity; M: motion; T: turbulence; W: wind]

Source	df	MS	*F*	*p*
C	2,12	0.493	3.60	
M	1,6	.033	.71	
T	1,6	.699	13.36	0.0106
W	2,12	.031	2.50	
CM	2,12	.015	.53	
CT	2,12	.127	6.08	.0151
CW	4,24	.031	1.61	
MT	1,6	.014	.58	
MW	2,12	.030	1.61	
TW	2,12	.010	.54	
CMT	2,12	.008	.71	
CMW	4,24	.016	.68	
CTW	4,24	.012	.52	
MTW	2,12	.107	.47	
CMTW	4,24	.018	1.00	

Table VIII. Results of ANOVA Test on SWAT Ratings

[C: task complexity; M: motion; T: turbulence; W: wind]

Source	df	MS	*F*	*p*
C	2,12	34 425	39.95	0.0000
M	1,6	681	5.80	.0527
T	1,6	4 250	19.93	.0043
W	2,12	1 420	8.21	.0057
CM	2,12	31	.42	
CT	2,12	834	3.46	
CW	4,24	723	4.96	.0047
MT	1,6	441	6.15	.0475
MW	2,12	36	.36	
TW	2,12	252	.99	
CMT	2,12	32	.43	
CMW	4,24	186	1.25	
CTW	4,24	164	1.06	
MTW	2,12	52	.46	
CMTW	4,24	74	.89	

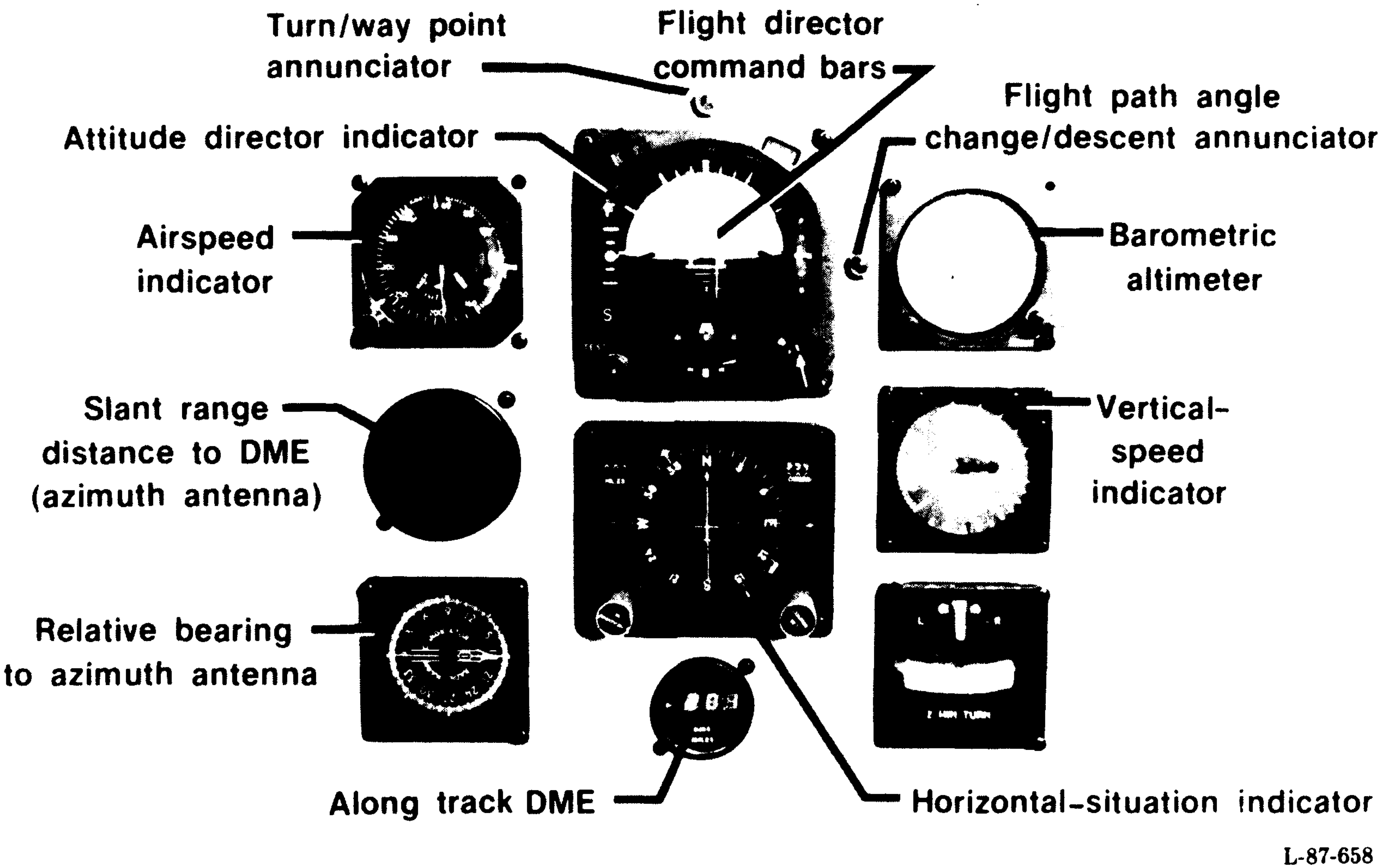

Figure 1. Flight instrumentation.

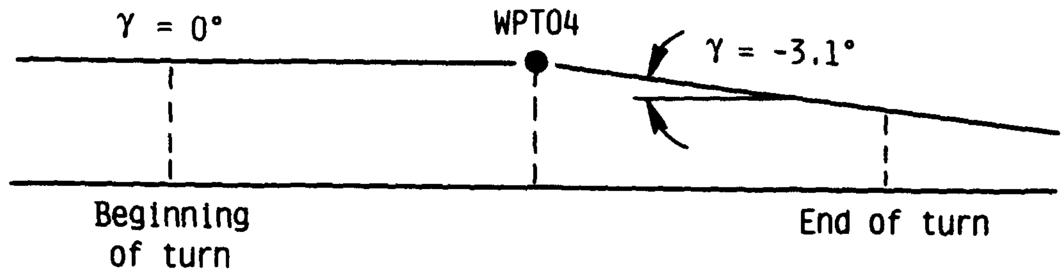

(a) Vertical view.

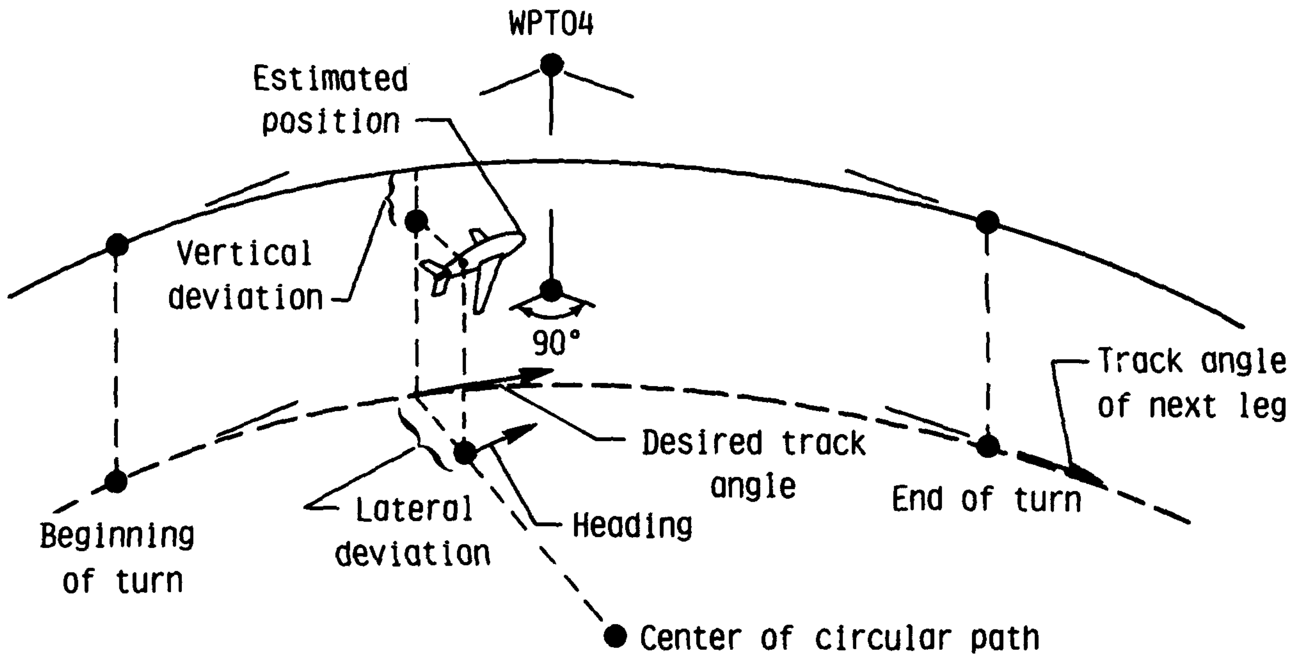

(b) Oblique view.

Figure 2. Circular path with fixed-radius guidance.

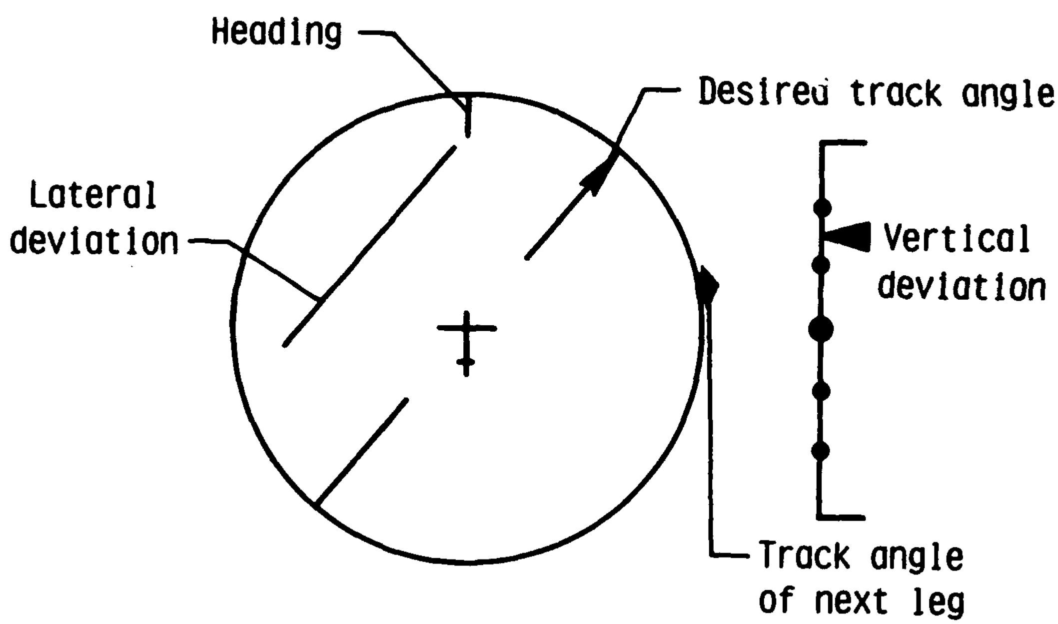

(c) Horizontal-situation indicator.

Figure 2. Concluded.

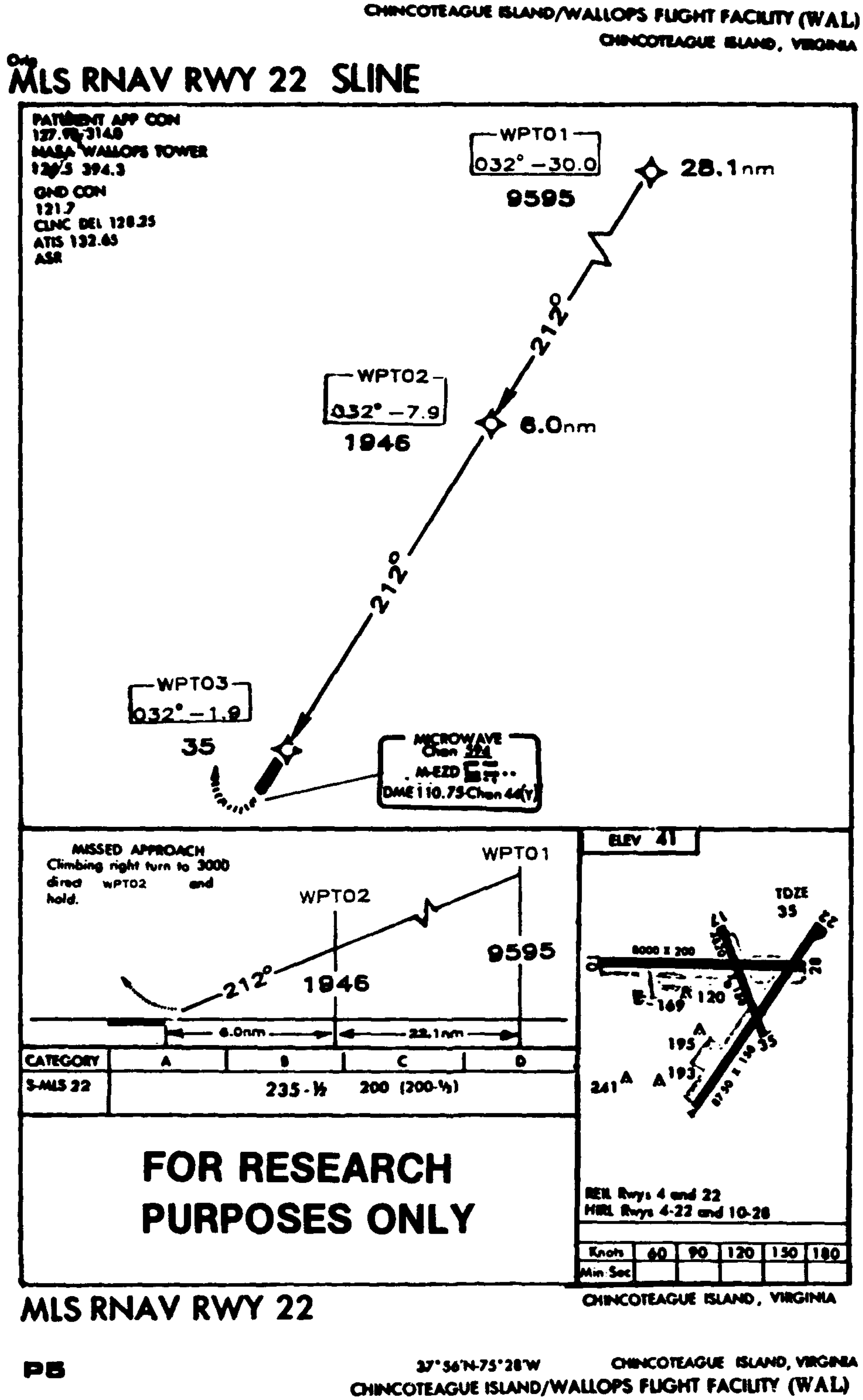

Figure 3. Geometry of straight-line, low-complexity approach task (SLINE).

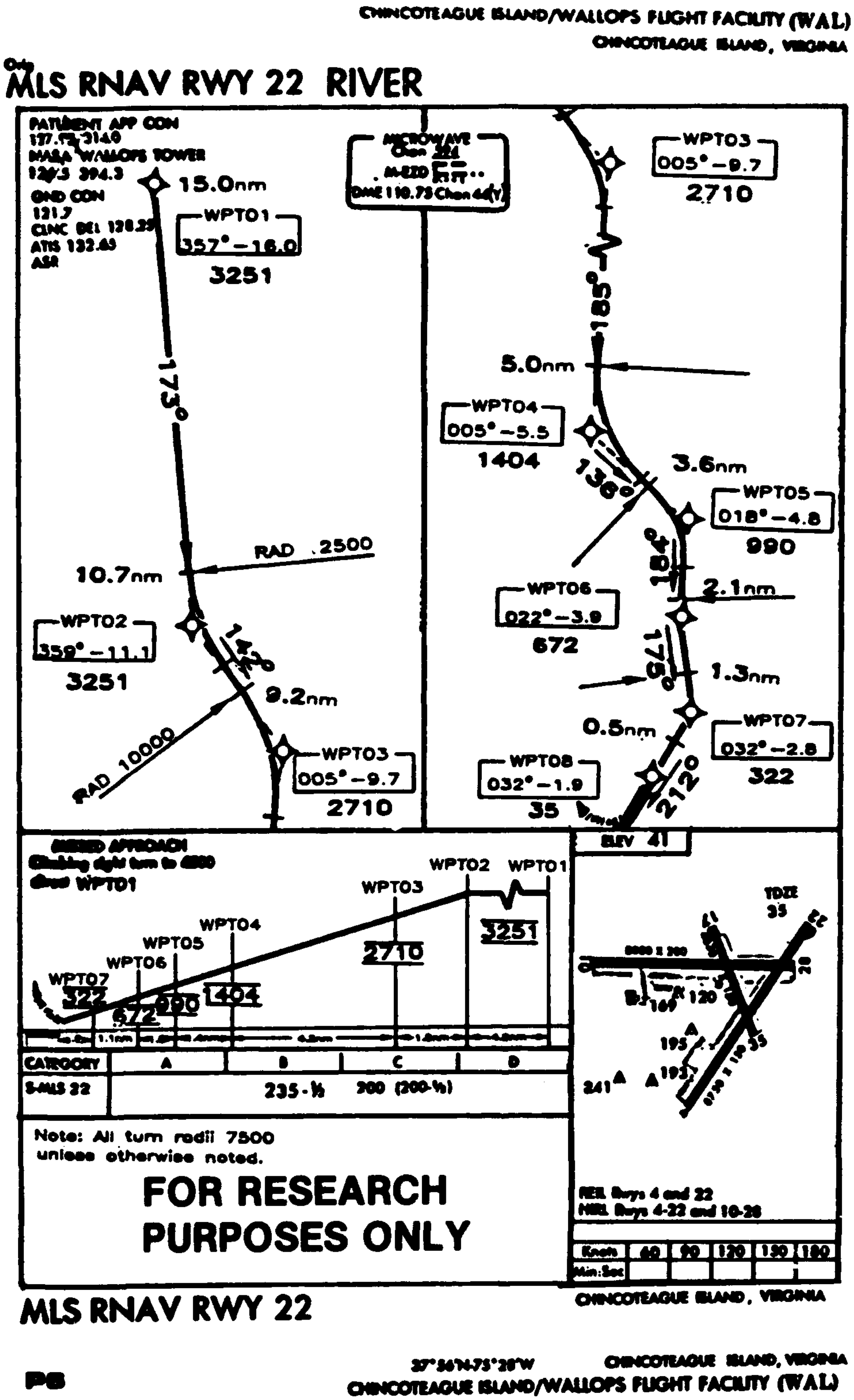

Figure 4. Geometry of medium-complexity approach task (RIVER).

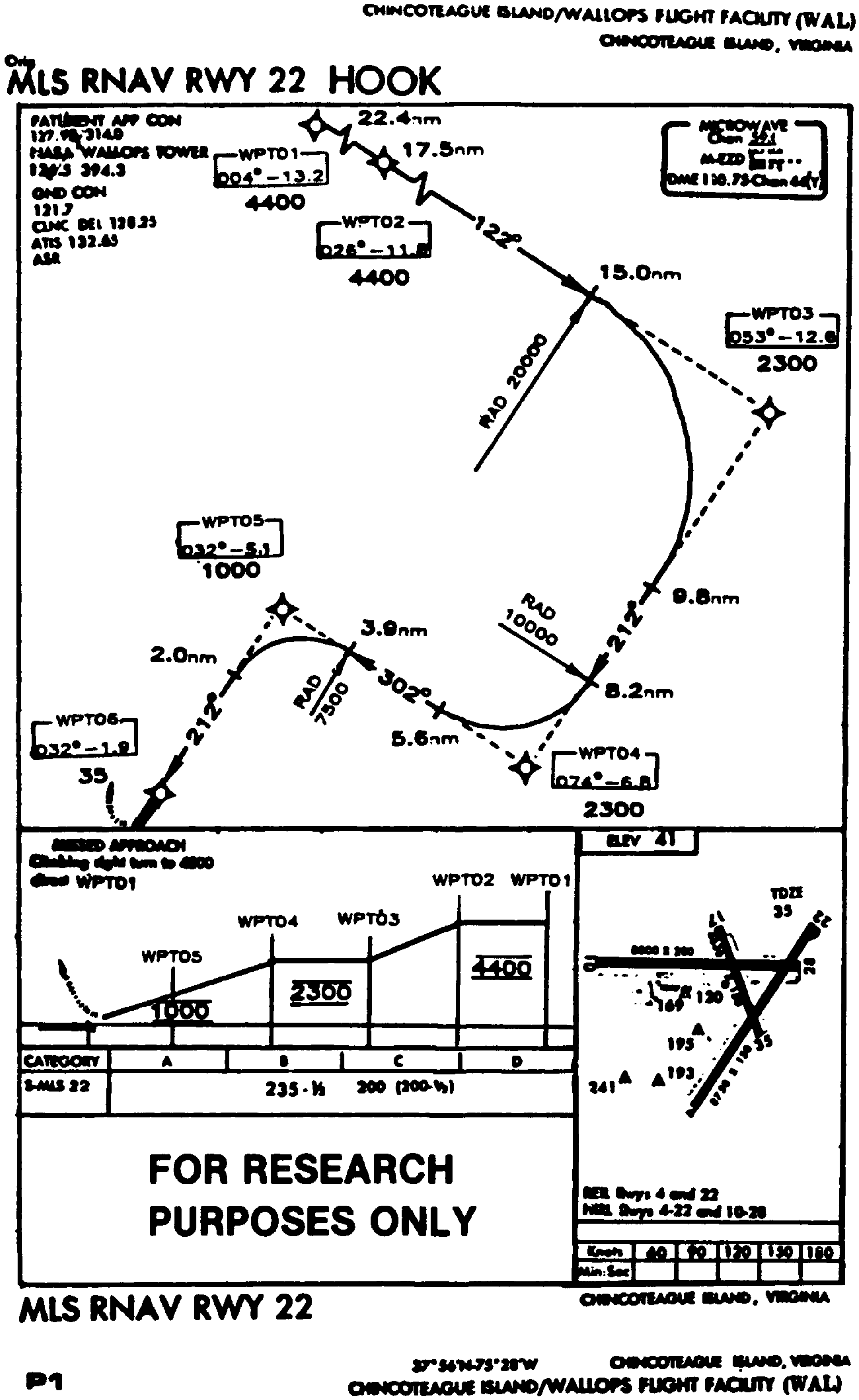

Figure 5. Geometry of high-complexity approach task (HOOK).

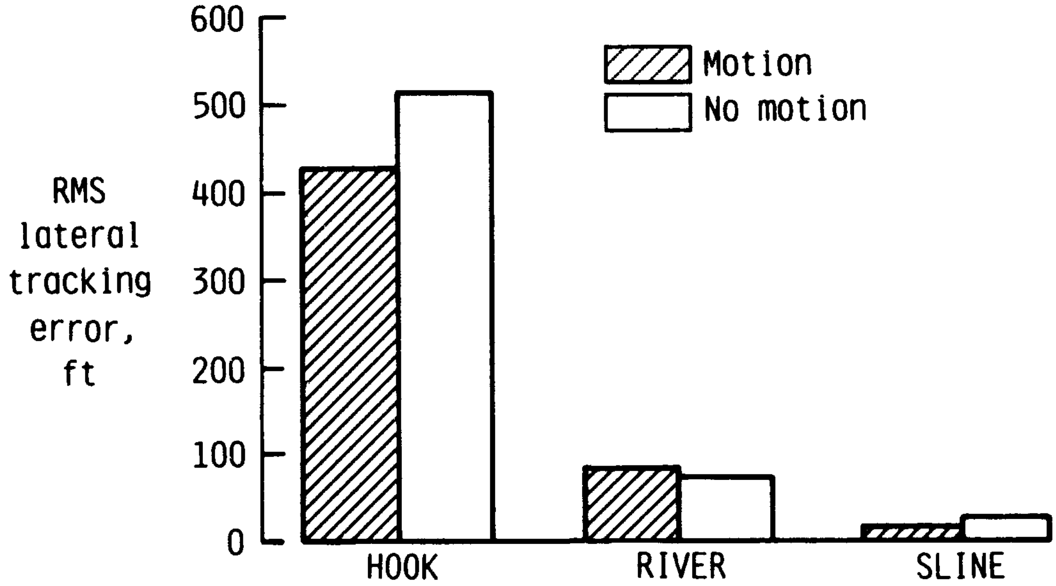

Figure 6. Lateral tracking error versus approach path complexity.

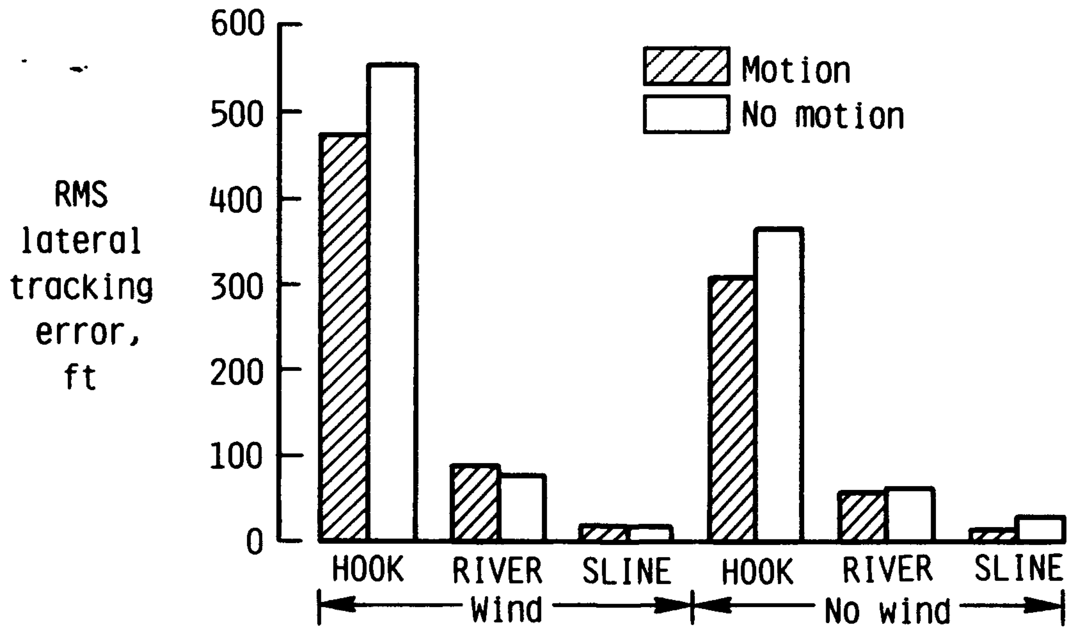

Figure 7. Lateral tracking error versus wind.

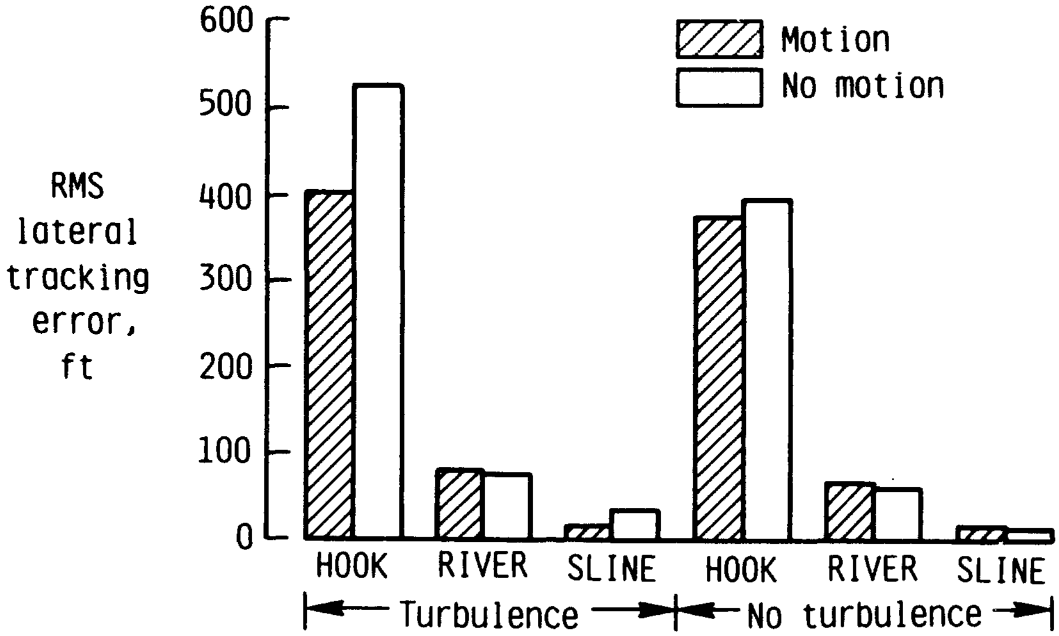

Figure 8. Lateral tracking error versus turbulence.

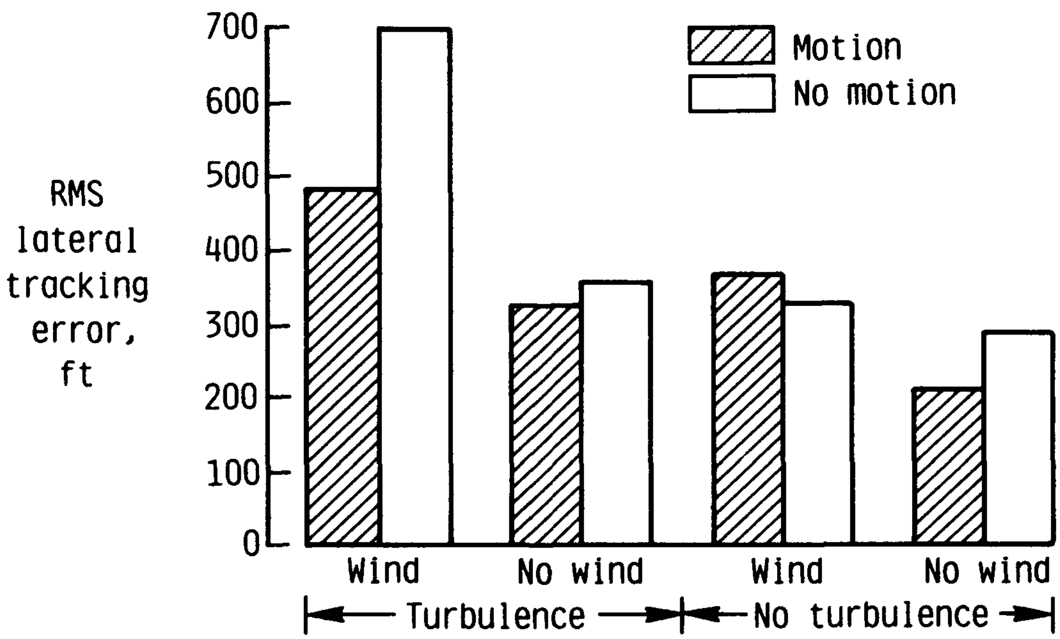

Figure 9. Lateral tracking error versus wind and turbulence for HOOK approach.

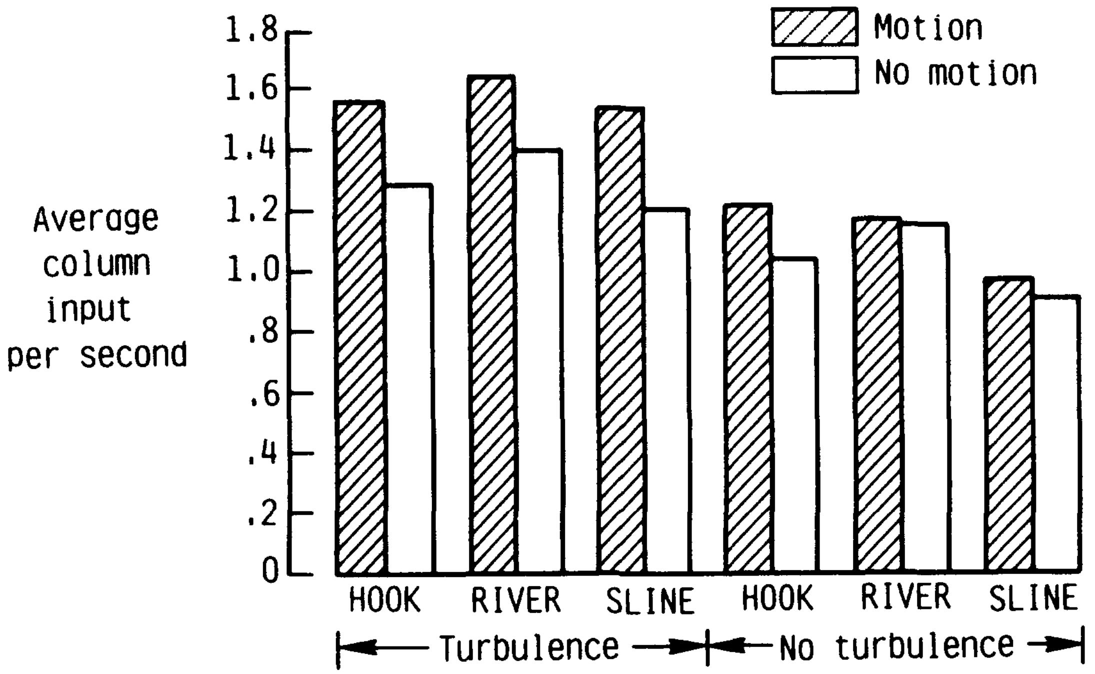

Figure 10. Column-input rate versus turbulence.

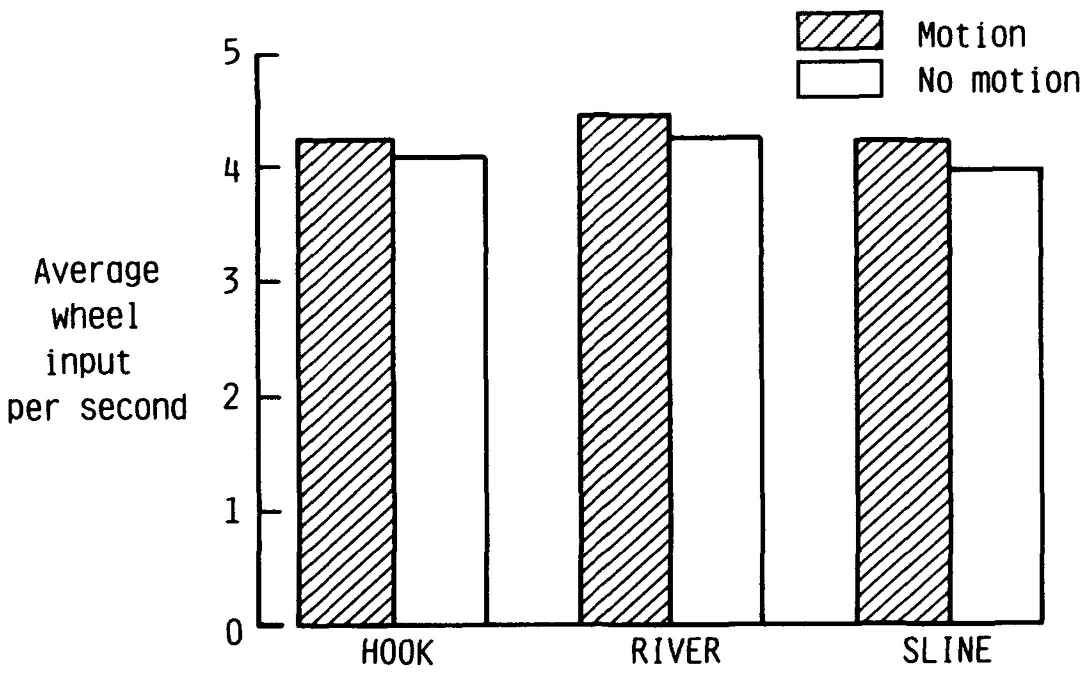

Figure 11. Wheel-input rate versus approach task complexity.

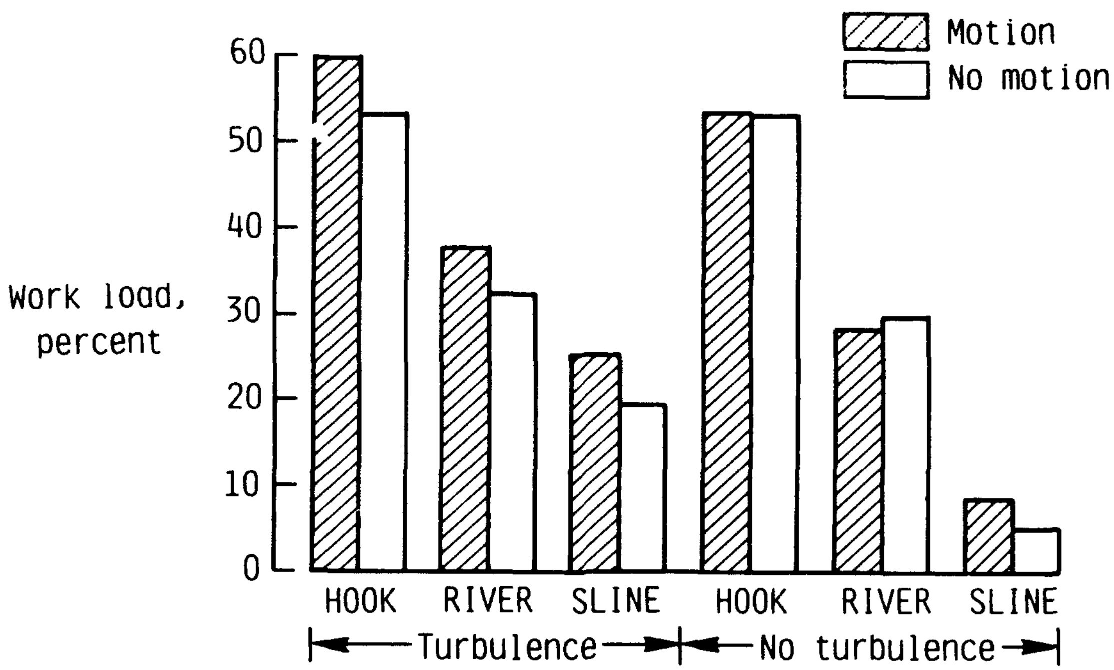

Figure 12. SWAT rating versus turbulence and task.

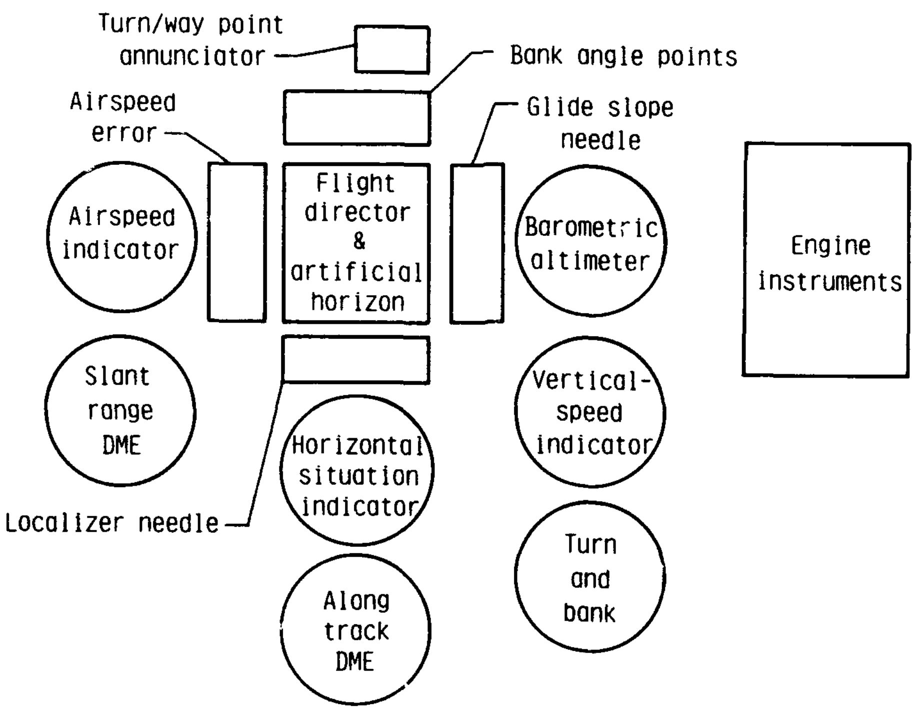

Figure 13. Oculometrically defined instrument look areas.

NASA
National Aeronautics and Space Administration

Report Documentation Page

1. Report No. NASA TP-2773	2. Government Accession No.	3. Recipient's Catalog No.
4. Title and Subtitle Effect of Motion Cues During Complex Curved Approach and Landing Tasks A Piloted Simulation Study		5. Report Date December 1987
		6. Performing Organization Code
7. Author(s) Charles H. Scanlon		8. Performing Organization Report No. L-16351
9. Performing Organization Name and Address NASA Langley Research Center Hampton, VA 23665-5225		10. Work Unit No. 505-66-41-57
		11. Contract or Grant No.
12. Sponsoring Agency Name and Address National Aeronautics and Space Administration Washington, DC 20546-0001		13. Type of Report and Period Covered Technical Paper
		14. Sponsoring Agency Code

15. Supplementary Notes
Research was done under cooperative agreement NCC1-107 between Arkansas State University and the Langley Research Center.

16. Abstract
A piloted simulation study was conducted to examine the effect of motion cues using a high-fidelity simulation of a commercial airplane during the performance of complex curved approach and landing tasks in the signal environment of the microwave landing system (MLS). The data from these tests indicate that in a high-complexity MLS approach task with moderate turbulence and wind, the pilot uses motion cues to improve path tracking performance. No significant differences in tracking accuracy were noted for the low- and medium-complexity tasks, regardless of the presence of motion cues. Higher control-input rates were measured for all the tasks when motion was used. Pilot eye scan, as measured by instrument dwell time, was faster when motion cues were used regardless of the complexity of the approach tasks. A pilot subjective rating, based on time, mental effort, and psychological stress loads, yielded larger work load ratings with motion than with no motion. Pilot comments indicated a preference for motion. With motion cues, pilots appeared to work harder in all levels of task complexity and to improve tracking performance in the most complex approach task.

17. Key Words (Suggested by Authors(s)) Simulator motion Work load Complex approach paths		18. Distribution Statement Unclassified—Unlimited Subject Category 05	
19. Security Classif.(of this report) Unclassified	20. Security Classif.(of this page) Unclassified	21. No. of Pages 25	22. Price A02

NASA FORM 1626 OCT 86 NASA-Langley, 1987

For sale by the National Technical Information Service, Springfield, Virginia 22161-2171